

Fuzzy Logic Based Controller Effective Energy Management Of Composite Energy Storage System Involving Battery And Ultracapacitor in Microgrid

Md.Asif¹, T.Thirumalkumar², D.Shobha Rani³, B.Ramu⁴, P.Harika⁵
^{1, 2, 3, 4, 5}(EEE, Vardhaman College of Engineering (Autonomous), JNTU, Hyderabad, India)

Abstract: In present world usage of fossil fuels are increasing, in order to decrease them the alternate option is Renewable-energy-based microgrids, they are a better way of utilizing renewable power and reduce the usage of fossil fuels. Usage of energy storage becomes mandatory when such microgrids are used to supply quality power to the loads. Microgrids have two modes of operation, namely, grid-connected and islanding modes. During islanding mode, the main responsibility of the storage is to perform energy balance. During grid-connected mode, the goal is to prevent transmission of the renewable source intermittency and load fluctuations to the grid. Energy storage of a single type cannot perform all these jobs efficiently in a renewable powered microgrid. The alternating nature of renewable energy sources like photovoltaic (PV) demands usage of storage with high energy density. At the same time, quick fluctuation of load demands storage with high power density. This paper shows a composite energy storage system (CESS) that contains both high energy density storage battery and high power density storage ultracapacitor to meet the aforesaid requirements. By using DAB power converter configuration and the energy management scheme can actively distribute the power demand among the different energy storages. Using fuzzy logic controller

Keywords: Bidirectional converter, energy management, energy storage, interleaved modulation, modular design and micro grid.

I. Introduction

Due to the intermittent nature of renewable energy sources and the incessant variations of the load, storage (e.g., battery, ultracapacitor, flywheel etc.) is usually needed in a renewable powered microgrid. The renewable output power profile and the load profile are two important factors in deciding the capacity and type of the energy storage components. The variation in output power from a utility-scale PV system is presented in fig [1],

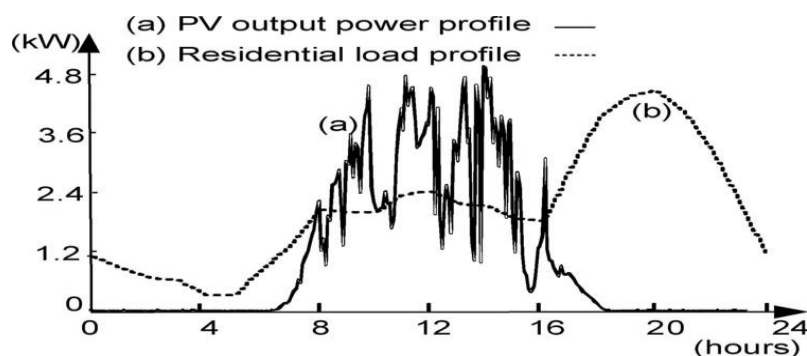


Fig. 1. Typical 24-h (a) PV output power and (b) residential load profile

From the fig 1 we can observe that variations in the pv output power profile comparing to residential load profile ,in order to compensate the pv output power with residential load profile we require Composite energy storage system (CESS) which includes battery and ultracapacitor , If we use only ultracapacitor, then it has to be oversized for storing large amount of energy to take care of the intermittency of the renewable sources and loads. Hence, use of a Composite energy storage system (CESS) encompassing both high power density and high energy density storage units is practically necessary. Now, the selection of the type of storage is also crucial.

For energy storage in the high power range for standard power systems, the most suitable ones would be pumped hydro storage, compressed air storage, etc.

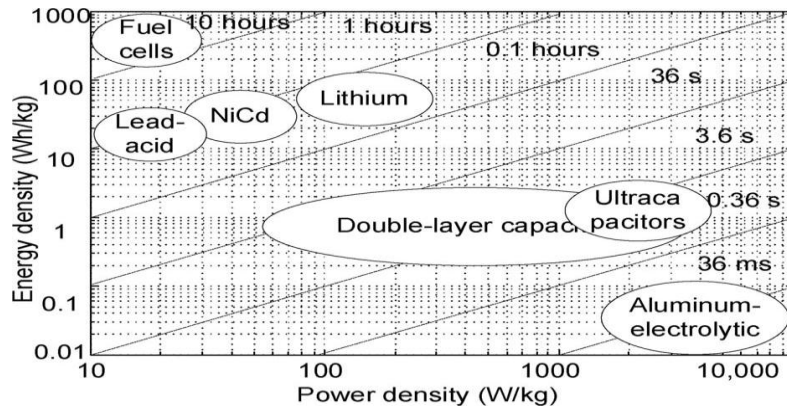


Fig. 2. Ragone chart showing the power density and energy density of different Storages.

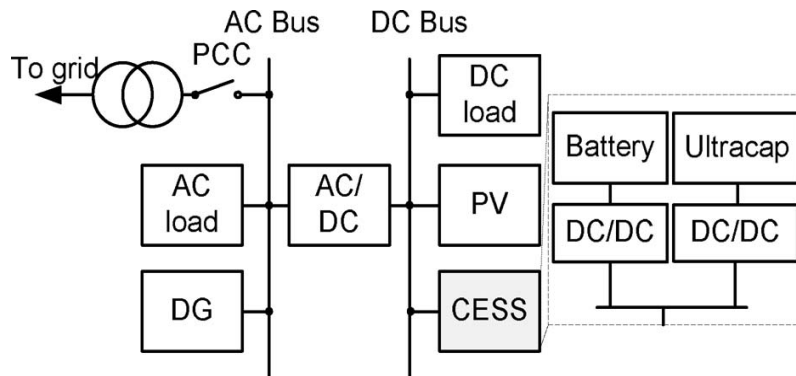


Fig. 3. Block diagram showing CESS interface with the dc grid.

However, for microgrids, where power levels are in the range of a few megawatts, battery, ultracapacitor, and flywheel are the more suitable options. Battery and ultracapacitor are considered as high energy density storage and high power density storage, respectively, and their combination is a very promising option to realize the CESS system. Fig 3 shows that ultracapacitor–battery hybrid energy storage performs better

than battery-alone energy storage for a stand-alone PV system.. fig 4 shows that battery–ultracapacitor hybrid storage has the virtues of both high energy density and high power

density, and also, such system increases battery life. .fig 5 analytically proved that battery–ultracapacitor hybrid achieves power and life extension of battery. This paper also exploits the potential of battery and ultracapacitor as a CESS, as shown in Fig. 3. Bidirectional dc–dc converters are required to interface the battery banks and the ultracapacitor to the dc link for controlling the power flow. The basic requirement from the dc–dc converter is that the user should be able to dynamically allocate the load current demand between the battery and the ultracapacitor. Different power converter structures are proposed in the literature for interfacing battery and ultracapacitor to the dc link. Fig 6 proposed that an ultracapacitor with a boost chopper can be connected to the terminals of the battery, and battery current can be indirectly controlled by controlling the ultracapacitor current. fig 7 proposed a technique, where ultracapacitor is connected to the battery with reduced power device rating.

The salient features of the proposed CESS system are:

- 1) dynamic allocation of steady power demands and transient power demands to the batteries and ultracapacitor, respectively;
- 2) flexible distribution of power flow among different batteries without disturbing the normal operation and online battery

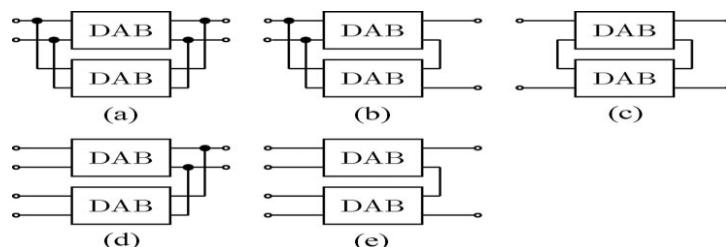
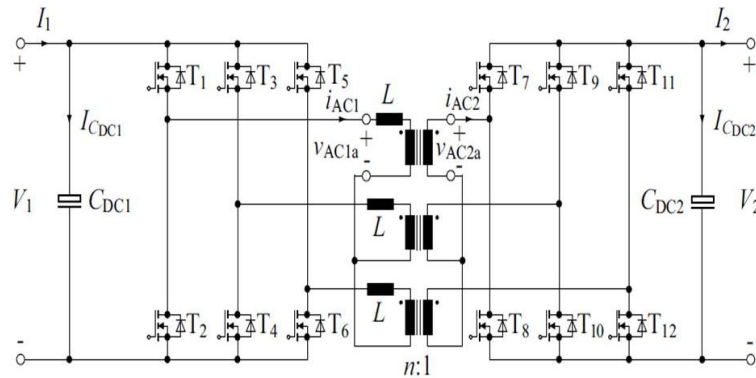


Fig. 4. Few possible configurations of module-based converter.

- (a) IPOP. (b) IPOS. (c) ISOS. (d) Modified version of IPOP.
- (e) Modified version of IPOS.replacement;
- (3) ultracapacitor charging–discharging without disturbing the normal operation; and
- (4) flexibility to upgradethe power rating or energy rating of the CESS systemindependently.

Incorporation of these features has been possiblebecause of the proposed unique modular power converterstructure.

II. Usage of Dab Converters



Three-phase Dual Active Bridge (DAB) converter topology.

As mentioned earlier, module-based design is the best approach to satisfy all the requirements of energy storage and load. The configurations of module-based converter are shown in Fig. 4. Input parallel output parallel (IPOP) configuration, as shown in Fig. 4(a), shares the input and output current in modules. By controlling the input current in each of the converters, the power flow in each can be controlled. Fig. 4(d) is derived from Fig.

4(a) to interface multiple sources. This is also a common topology in connecting multiple sources [18]. Input parallel output series (IPOS) topology presented in Fig. 4(b) shares the current in the parallel side, while achieves high voltage in the series side. Therefore, it is suitable for applications, where energy storage and load have large voltage difference. Fig. 4(e) is derived from Fig. 4(b) to interface multiple sources. Input

Series output series (ISOS) configuration of Fig. 4(c) shares voltage both in input and output side. It is favorable for high input and output voltage application. This connection is especially useful when power increases to megawatt level, since higher voltage can help to reduce the magnitude of current to achieve lower loss. In all the aforementioned schemes, the basic power converter module used is the DAB. The module-based converter design approaches not only can match the different source and load requirements, but also share the power in each module, and thus help to reduce the switch stress. Table. I lists the comparison of switch stress and transformer turns ratio in IPOP, IPOS, and ISOS

TABLE I
Comparison of Device Stress under Same Output Power

	IPOP (p.u.)	IPOS (p.u.)	ISOS (p.u.)
Primary			
Switch Current Rating	1/n	1/n	1
Switch Voltage Rating	1	1	1/n
Secondary			
Switch Current Rating	1/n	1	1
Switch Voltage Rating	1	1/n	1/n
Turns ratio	1	1/n	1

With single DAB converter, respectively. Base values are chosen according to single DAB rating when same power and same input/output voltage are used. From Table. I, we can clearly see the advantages of different topologies in switch rating selection. For example, the current rating for primary-side switches and voltage rating for the secondary-side switches are reduced to 1/n p.u. (as shaded rows) when n modules are connected

under IPOS structure. This modular design approach is followed in realizing the power converter structure in the proposed CESS system.

III. Proposed Power Converter Structure

The ultracapacitor needs to supply or absorb high current for a short duration of time. Considering these requirements, the modular power converter structure adopted for interfacing battery and ultracapacitor to the dc bus is shown in Fig. 5. The added advantage of such modular structure is that if n parallel DAB branches are used, then by applying the interleaving scheme, the input-current and output-voltage ripple frequency can be increased by a factor of n and ripple magnitude can be reduced to less than $1/n$ compared to single DAB. At this point, it is important to explore the reconfigurability of the proposed modular power converter structure of Fig. 5.

If the energy density of the CESS needs to be increased, then we can add parallel branches to the battery side, as shown in Fig. 5. High energy density may be required, if the microgrid is powered from only renewable sources. Similarly, more ultracapacitor branches can be added to increase the power density of CESS. High power density may be required for CESS used in traction application, where high burst of power is supplied or absorbed during acceleration or braking, respectively. Moreover, the power converter structure can be easily reconfigured to achieve different dc-link voltage levels, as shown in Fig. 6

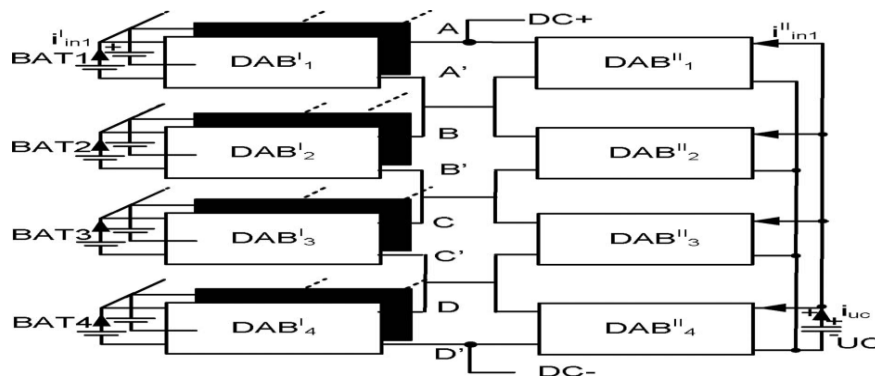


Fig. 5. Topology of the proposed interleaved DAB-based CESS.

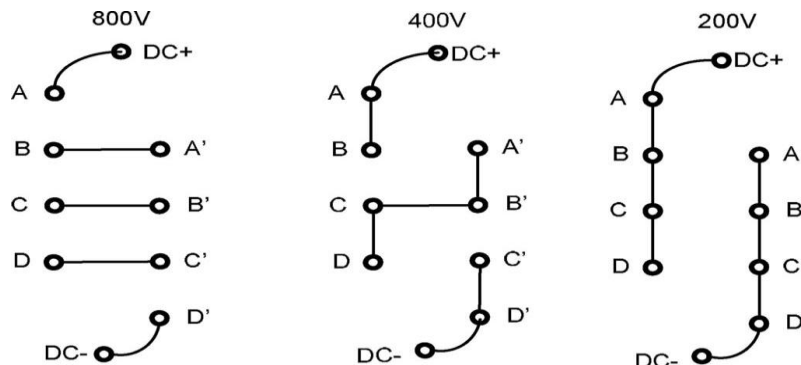


Fig. 6. Reconfiguration of the power converter structure to satisfy different dc-link voltage requirements.

IV. Proposed Control Strategy Of Dabs For Energymanagement Of The Cess System

The control scheme for energy management of this CESS system is shown in Fig. 7. The symbols used to represent different variables are defined in the Appendix. DAB converter is selected as a basic cell in our application. The power transfer is achieved by phase shifting the voltage across the primary and secondary sides of the high-frequency transformer. The detailed operating principles of DAB is explained in . Every DAB has a current-control loop associated with it. The output of the current controller generates the phase-shift information between the input and output bridges of the DAB module. The task of the energy management block of CESS is to generate appropriate current reference for each DAB module. For the analysis, the direction of current flowing out of battery and ultracapacitor is taken as positive, as shown in Fig. 5.

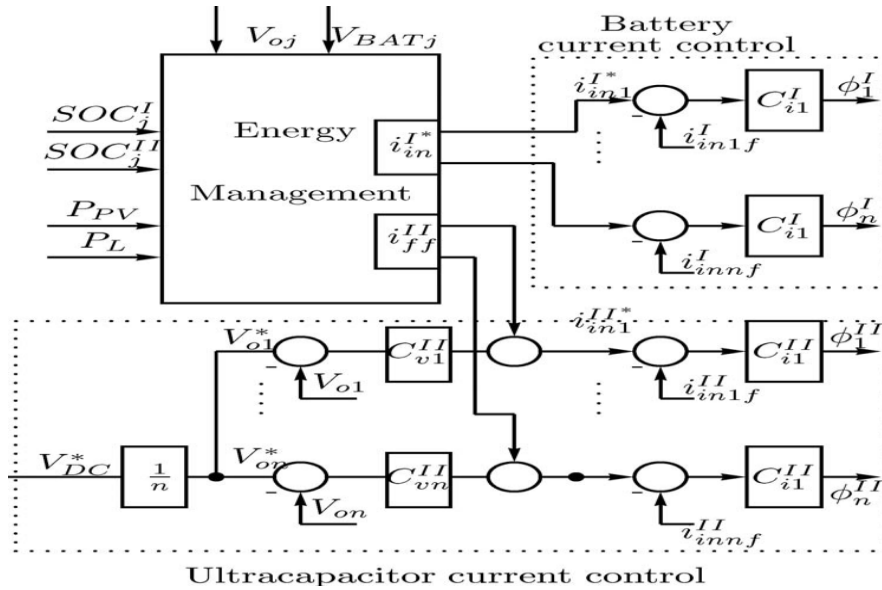


Fig. 7. Control block diagram for the IPOS interleaved DAB converter.

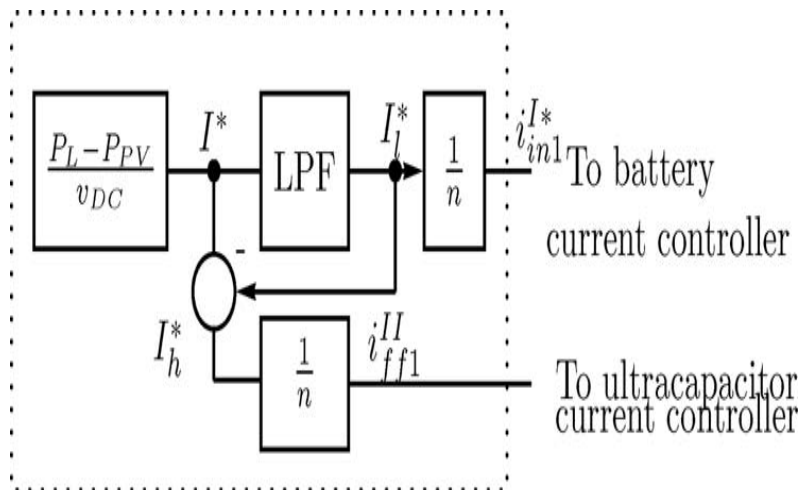
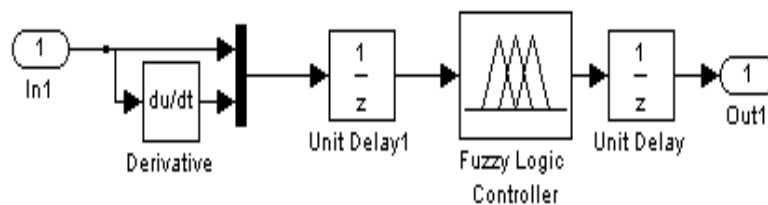


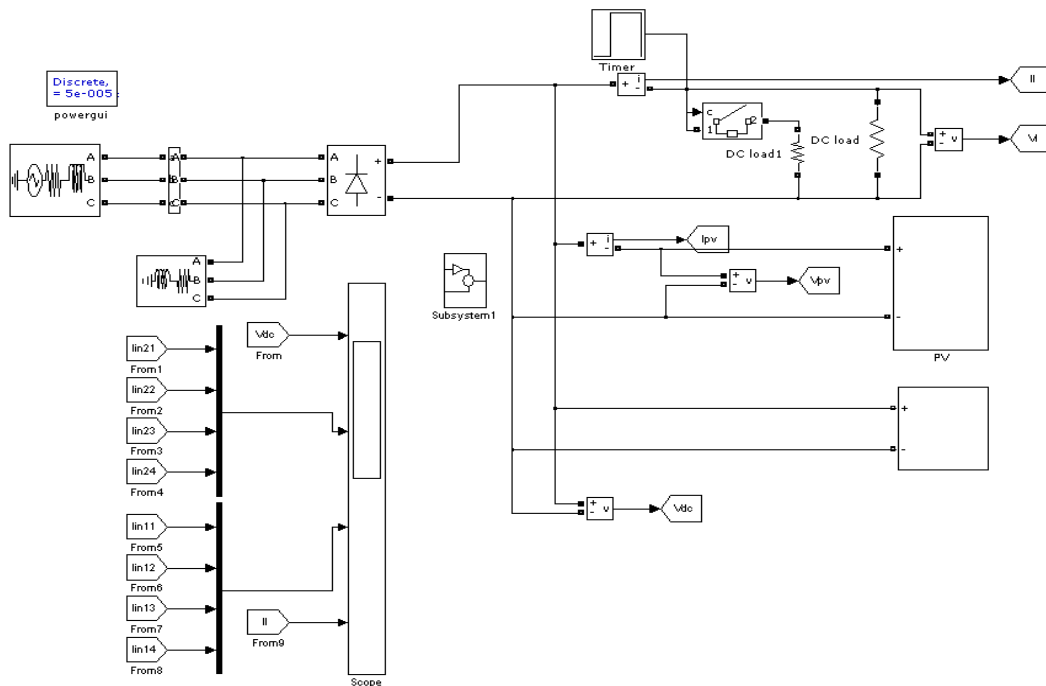
Fig. 8. Energy management strategy for case I.

V. Output Simulation Result

Simulation result of Based On Fuzzy Logic Controller Effective Energy Management In Composite Energy Storage System Involving Battery And Ultracapacitor In Microgrid Applications



Using Fuzzy Logic Controller at Subsystem



A. Case I: Dynamic Allocation of Power Demand to Batteries and Ultracapacitor

One objective of the energy management system is to allocate steady power demand to the batteries and transient power demand to the ultracapacitor. We can think of a specific example of a dc grid, where PV generator and load are connected along with the CESS system. The block diagram of the overall control scheme is shown in Fig. 7, and the current reference generation strategy for this specific case is shown in Fig. 8. The total current demand from the CESS system is calculated depending on the difference between energy source power and load power. Here, the current demand can be positive or negative depending on the difference. Then, this current reference is passed through a low-pass filter (LPF) to get the low-frequency component of the current demand. This low-frequency component $I^* l$ is used to generate the total current reference for the battery interfacing power converters. As there are n parallel DAB branches, the current reference for each branch would be $I^* l / n$. In this case, it is assumed that, all the batteries are at the same state of charge (SOC). For controlling the DABs interfacing the ultracapacitor, a cascaded control scheme using inner current-control loop and outer voltage-control loop is realized. The high-frequency component of the current demand from the CESS system is added as feedforward term at the output of the voltage controllers. The value of this feedforward term for each DAB branch is equivalent to $I^* h / n$. To verify this control strategy, simulation is carried out in SIMPLORER software.

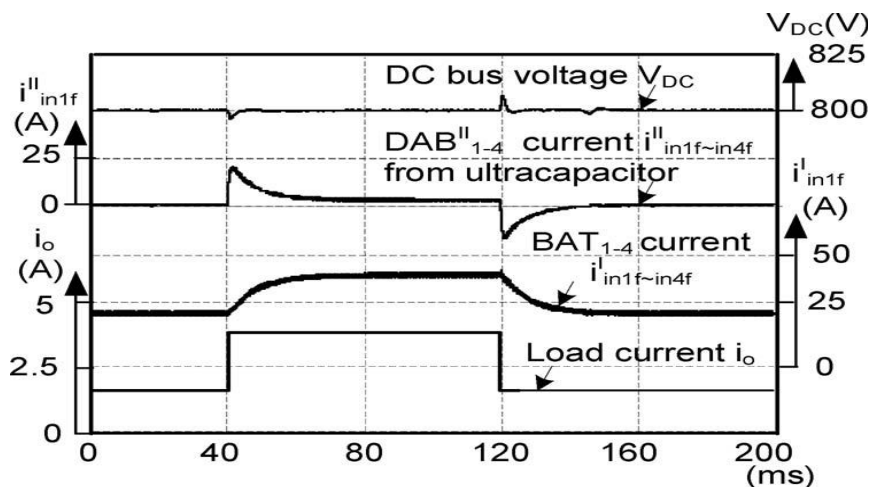


Fig. 9. Dynamic response for a step change in current demand from the CESS system (Case I).

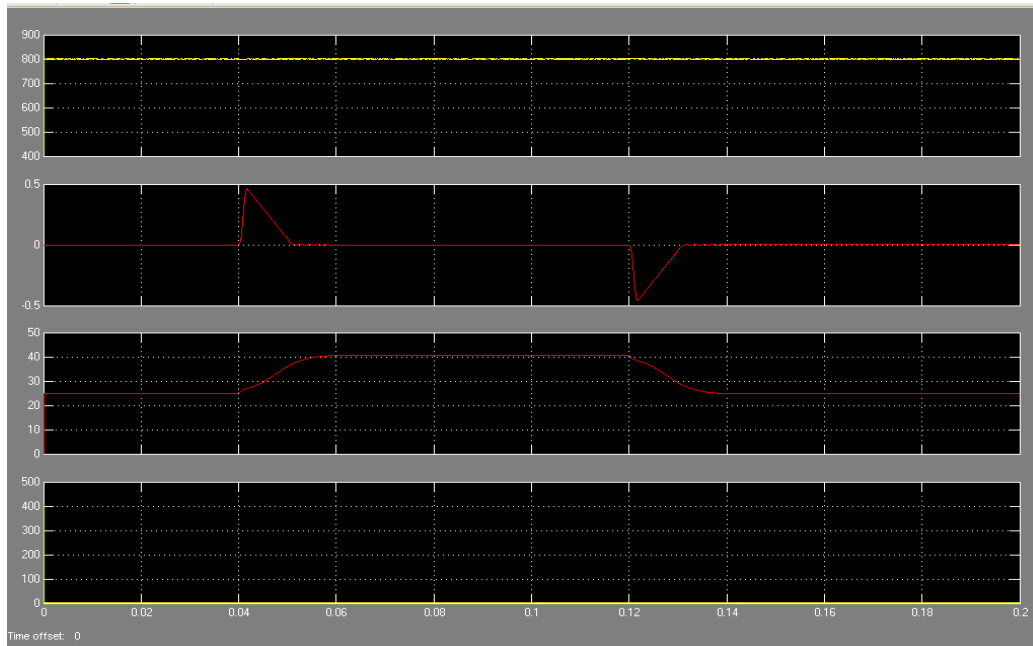


Fig. 9.1. Output simulation result of Case I: Dynamic Allocation of Power Demand to Batteries and Ultracapacitor

Four parallel branches are considered. Each branch is rated for 1.2 kW. In order to justify the scheme in a practical scenario, upto 20% variation in leakage inductance and output capacitance are considered. Fig. 9 shows the dynamic response of the dc-link voltage and the average converter input currents for step variation in current demand from the CESS system. In practice, a sudden variation in current demand can occur for switching ON or switching OFF some particular load or for sudden change in solar insolation because of passing clouds. At $t = 40$ ms, there is a step increase in the load current. It is evident from Fig. 9 that ultracapacitor-interfacing converter currents $i_{ii}(1f-4f)$ compensates for the sudden current dynamics, and the battery currents $i_{ii}(1f-4f)$ slowly increases to cater to the steady load demand. The time constant of the LPF shown in Fig. 8 is kept as only 50 ms to show the operating principle. In practice, this cutoff frequency has to be set depending on the relative capacity of the battery and ultracapacitor. Similar response can be seen for a step decrease in load current at $t = 120$ ms.

B. Case II: Energy Management of the Batteries

In an ideal case, all the batteries can source or sink same current. But in practice, different batteries will be in different states of charge and their equalization is required. In the example of the earlier section, the current reference for all the batteries are set equal as $I \cdot 1/n$. However, the energy management scheme can actually allocate different current references for different batteries depending on their states of charge. Fig. 10(a) shows that if same current is drawn from all the four batteries with only one of them having higher SOC, then batteries with lower SOC can go into deep discharge. Hence, if we put a deep discharge limit, then the energy stored in the battery with higher SOC cannot be fully utilized. In fact, this result also indirectly explains that, if many batteries are connected in series to form a high-voltage dc-link, then volumetric efficiency of the battery bank will be decided by the battery with lowest SOC, resulting in reduced energy density. However, if current drawn from individual batteries is proportional to their individual SOC, then all the batteries will hit the deep discharge limit together and their energy can be fully utilized as shown in Fig. 10(b). In this case, the battery with higher SOC supplies more current till all the batteries reach same SOC. The authors in [19] and [20] ex-

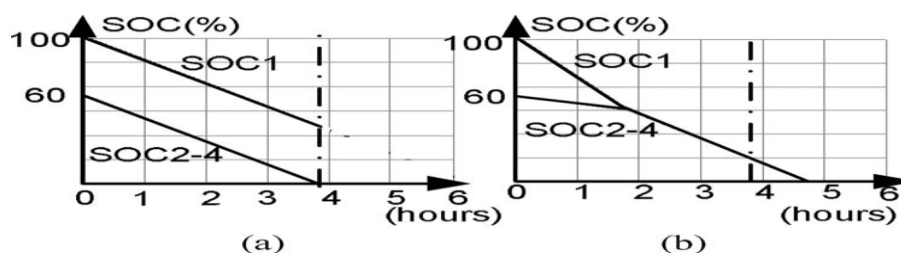


Fig. 10. SOC of all the batteries (a) with equal discharge current and (b) with their discharge current proportional to their SOC.

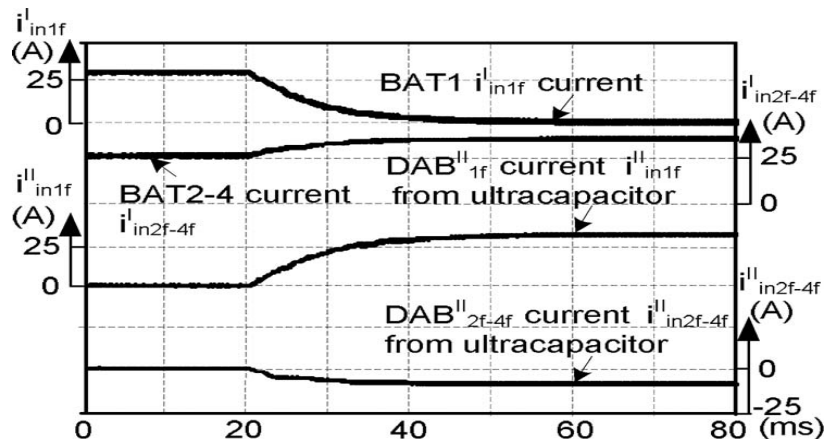


Fig. 11. Dynamic response of converter currents when one battery current reference is made zero (Case II).

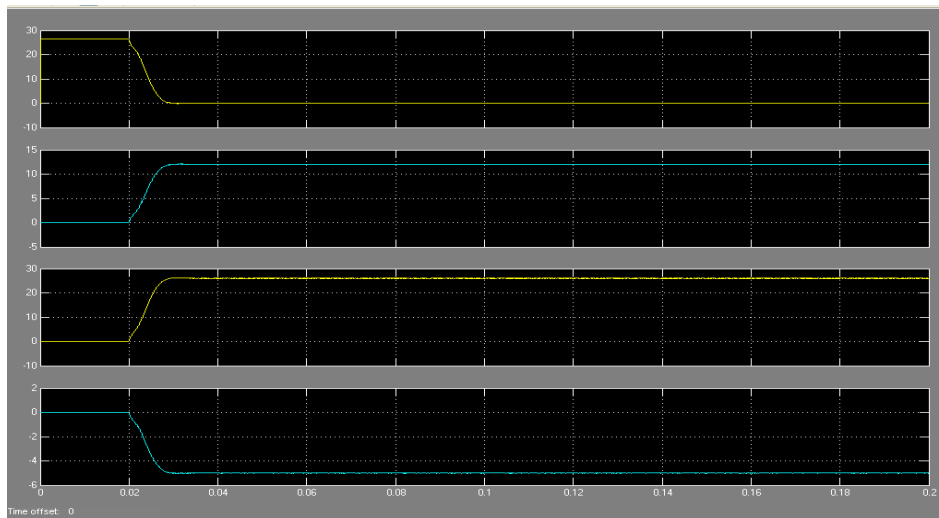


Fig. 11.. Output simulation result of Dynamic response of converter currents when one battery current reference is made zero (Case II).

plained the needs for SOC control and propose control methods for SOC balancing of the battery units. emphasized on power sharing among different batteries depending on their charge level and to achieve this, droop coefficient is adjusted to be inversely proportional to their charge level. One extreme case can be a situation when one of the battery currents has to be made zero to disconnect it for replacement. Fig. 11 shows the simulation results corresponding to this dynamics. The current reference to the DAB connected to the battery to be replaced is slowly made zero starting at $t = 20$ ms. The reduction of this battery power is compensated by other batteries by increasing their current references. The voltage controllers adjust the current references of the DABs connected to the ultracapacitor to regulate $V_o(1-4)$ at the reference value. Fig. 11 shows the dynamic response of the average converter input currents for letting one battery current i_{in1f} to become zero. The average currents $i_{in(2f-4f)}$ of converters connected to other batteries slowly increase to compensate. Because of this change in battery currents, the input current i_{in1f} of DAB I1 increases and input currents $i_{in(2f-4f)}$ of DAB II2-4 decrease to regulate the dc bus.

C. Case III: State of Charge Control of Ultracapacitor

The ultracapacitor SOC control is also an important requirement of the energy management scheme. The ultracapacitor SOC can be easily estimated from its terminal voltage. The energy management scheme has to maintain the ultracapacitor SOC within a band. If the ultracapacitor voltage falls below the lower band, then the energy management scheme generates appropriate current references for the battery and ultracapacitor.

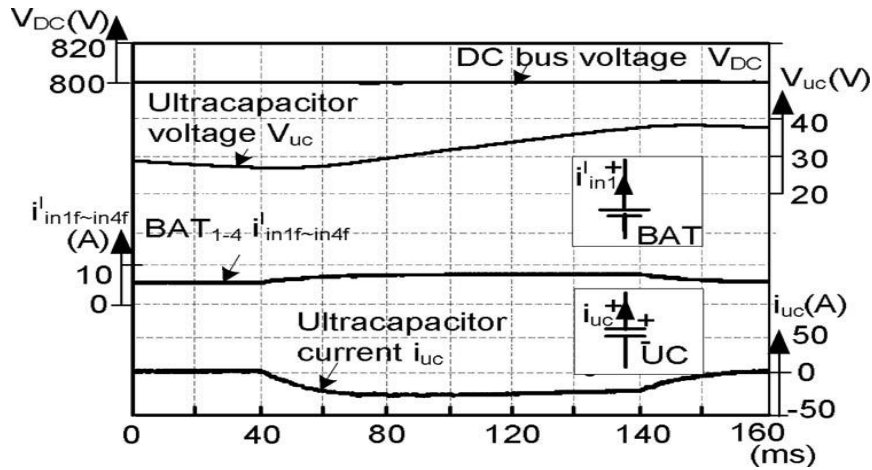


Fig. 12. Ultracapacitor charging scheme (Case III).

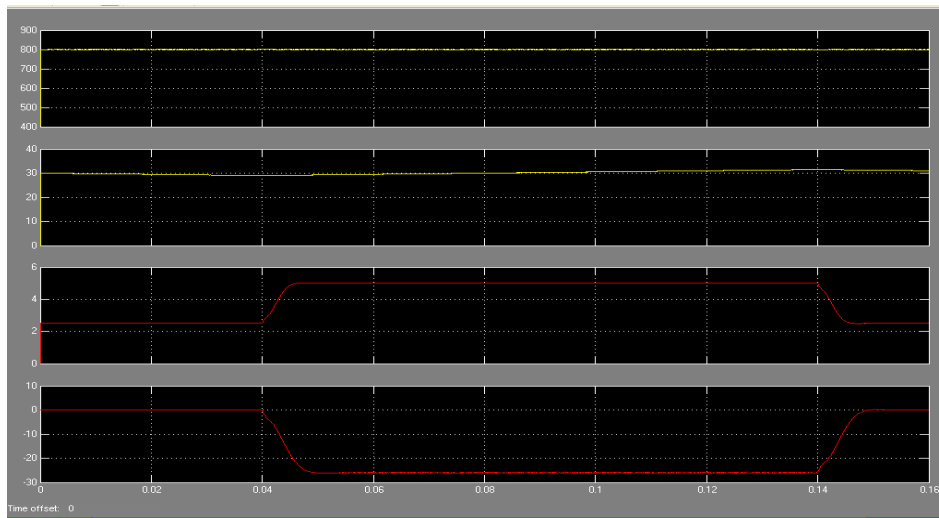


Fig. 12. Output simulation result of Ultracapacitor charging scheme (Case III).

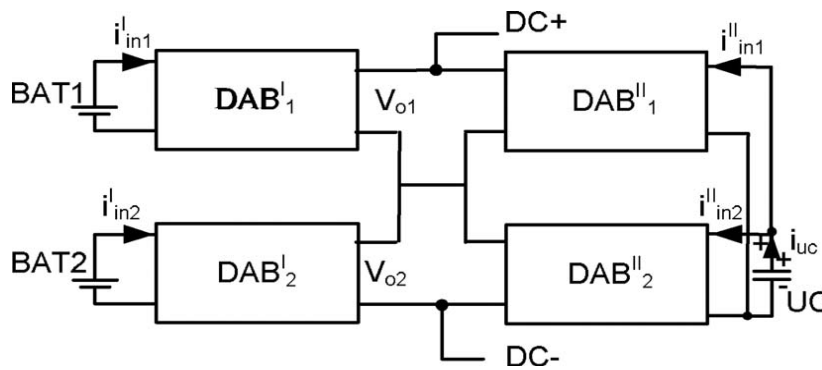


Fig. 13. Block diagram of the experimental setup.

The simulation results showing ultracapacitor charging processis presented in Fig. 12. For charging the ultracapacitor, a negativecurrent reference is added to the controllers of the DABsinterfacing it to the dc bus. Hence, the ultracapacitor currentbecomes negative, as shown in Fig. 12. To compensate for thisoutflow of current from the dc bus, a positive current referenceis added to the controllers of the DABs interfacing the batteriesto the dc bus. The resulting increase in magnitude of averagebattery currents $i_{in}(1f-4f)$ is shown in Fig. 12. Once the ultracapacitorgets charged, i.e., the ultracapacitor voltage V_{UC} reaches the upper band, this added offset current is removed. Fig. 12 shows that there is no disturbance in the dc-bus voltage V_{dc} throughout this process.

VI. CONCLUSION

This CESS interfaces battery as a high energy density storage, and ultracapacitor as a high power density storage to the dc bus. The dc–dc converter structure is formed using DAB modules whose terminals are connected in series or parallel depending on feasibility. The proposed modular dc–dc converter topology along with its energy management scheme can flexibly share the power between different batteries and ultracapacitor. This scheme is validated based on fuzzy logic controller simulation in this paper.

REFERENCES

Proceedings Papers:

- [1] A. E. Curtright and J. Apt, "The character of power output from utility scale photovoltaic systems," *IProg. Photovolt: Res. Appl.*, vol. 16, pp. 241–247, 2008.
- [2] T. Christen and M. Carlen, "Theory of ragon plots," *J. Power Sources*, vol. 91, no. 2, pp. 210–16, 2000.
- [3] M. Glavin, P. Chan, S. Armstrong, and W. Hurley, "A stand-alone photovoltaic supercapacitor battery hybrid energy storage system," in *Proc. 13th Power Electron. Motion Control Conf.*, 2008 (EPE-PEMC 2008), pp. 1688–1695.
- [4] Z. Guoju, T. Xisheng, and Q. Zhiping, "Research on battery supercapacitor hybrid storage and its application in microgrid," in *Proc. 2010 Asia-Pacific Power Energy Eng. Conf. (APPEEC)*, pp. 1–4.
- [5] R. Dougal, S. Liu, and R. White, "Power and life extension of battery ultracapacitor hybrids," *IEEE Trans. Compon. Packag. Technol.*, vol. 25, no. 1, pp. 120–131, Mar. 2002.
- [6] B. and P. , "Battery-ultracapacitor active parallel interface with indirect control of battery current," in *Proc. Power Energy Conf. Illinois (PECI)*, 2010, pp. 12–19.
- [7] G. Guidi, T. Undeland, and Y. Hori, "An optimized converter for battery supercapacitor interface," in *Proc. IEEE Power Electron. Spec. Conf. (PESC 2007)*, pp. 2976–2981.
- [8] W. Li and G. Joos, "A power electronic interface for a battery supercapacitor hybrid energy storage system for wind applications," in *Proc. IEEE Power Electron. Spec. Conf. (PESC 2008)*, pp. 1762–1768.
- [9] F. Garcia, A. Ferreira, and J. Pomilio, "Control strategy for battery ultracapacitor hybrid energy storage system," in *Proc. 24th Annu. IEEE Appl. Power Electron. Conf. Expo. (APEX 2009)*, pp. 826–832.
- [10] F. H. Khan and L. M. Tolbert, "Bi-directional power management and fault tolerant feature in a 5-kw multilevel dc-dc converter with modular architecture," *IET Trans. Power Electron.*, vol. 2, pp. 595–604, 2009.
- [11] L. Palma and P. N. Enjeti, "A modular fuel cell, modular dc-dc converter concept for high performance and enhanced reliability," *IEEE Trans. Power Electron.*, vol. 24, no. 6, pp. 1437–1443, Jun. 2009.
- [12] A. J. Watson, H. Dang, G. Mondal, J. C. Clare, and P. W. Wheeler, "Experimental implementation of a multilevel converter for power system integration," in *Proc. IEEE Energy Convers. Congr. Expo. (ECCE)*, Sep. 2009, pp. 2232–2238.
- [13] H. Zhou, T. Bhattacharya, and A. M. Khambadkone, "Composite energy storage system using dynamic energy management in microgrid applications," in *Proc. 2010 Int. Power Electron. Conf.*, Jun., pp. 1163–1168.
- [14] S. Inoue and H. Akagi, "A bidirectional isolated dc-dc converter as a core circuit of the next-generation medium-voltage power conversion system," *IEEE Trans. Power Electron.*, vol. 22, no. 2, pp. 535–542, Mar. 2007.
- [15] H. Zhou and A. M. Khambadkone, "Hybrid modulation for dual-active bridge bidirectional converter with extended power range for ultracapacitor application," *IEEE Trans. Ind. Appl.*, vol. 45, no. 4, pp. 1434–1442, Jul./Aug. 2009.
- [16] R. W. A. A. D. Doncker, D. M. Divan, and M. H. Kheraluwala, "A three-phase soft-switched high-power-density dc/dc converter for high-power applications," *IEEE Trans. Ind. Appl.*, vol. 27, no. 1, pp. 63–73, Jan./Feb. 1991.
- [17] W. Chen, R. Xinbo, Y. Hong, and C. K. Tse, "Dc/dc conversion systems consisting of multiple converter modules: Stability, control, and experimental verifications," *IEEE Trans. Power Electron.*, vol. 24, no. 6, pp. 1463–1474, Jul./Aug. 2009.
- [18] H. Zhou, A. M. Khambadkone, and X. Kong, "Fast dynamic response in a fuel cell based converter using augmented energy storage," in *Proc. IEEE Power Electron. Spec. Conf. (PESC 2007)*, Sep., pp. 1255–1260.
- [19] L. Maharjan and E. A. S. Inoue, "State-of-charge (soc)-balancing control of a battery energy storage system based on a cascade pwm converter," *IEEE Trans. Power Electron.*, vol. 24, no. 5, pp. 1628–1636, Jun. 2009.
- [20] W. Du, X. Huang, S. Yang, F. Zhang, X. Wu, and Z. Qian, "A novel equalization method with defective-battery-replacing for series-connected lithium battery strings," in *Proc. IEEE Energy Convers. Congr. Expo. (ECCE 2009)*, pp. 1808–1811.
- [21] J. Guerrero, J. Vasquez, J. Matas, M. Castilla, and L. de Vicuna, "Control strategy for flexible microgrid based on parallel line-interactive up systems," *IEEE Trans. Ind. Electron.*, vol. 56, no. 3, pp. 726–736, Mar. 2009.
- [22] D. Tran, H. Zhou, and A. M. Khambadkone, "Energy management and dynamic control in composite energy storage system for micro-grid applications," in *Proc. IEEE Ind. Electr. (IECON-2010)*, pp. 1818–1824.